

Temperature-dependent decay dynamics in highly mismatched ZnSe_{1-x}Te_x alloy

Yan-Cheng Lin, Wei-Shi Jiang, Wu-Ching Chou, Wei-Kuo Chen, Wen-Hao Chang, Chin-Hau Chia, Cheng-Yu Chen, and Jen-Inn Chyi

Citation: *Applied Physics Letters* **100**, 071912 (2012); doi: 10.1063/1.3687187

View online: <http://dx.doi.org/10.1063/1.3687187>

View Table of Contents: <http://scitation.aip.org/content/aip/journal/apl/100/7?ver=pdfcov>

Published by the *AIP Publishing*

Articles you may be interested in

[Recombination dynamics and carrier lifetimes in highly mismatched ZnTeO alloys](#)

Appl. Phys. Lett. **103**, 261905 (2013); 10.1063/1.4858968

[Role of heteroepitaxial misfit strains on the band offsets of Zn_{1-x}Be_xO/ZnO quantum wells: A first-principles analysis](#)

J. Appl. Phys. **111**, 113714 (2012); 10.1063/1.4729079

[Origin of the near-band-edge luminescence in Mg_xZn_{1-x}O alloys](#)

J. Appl. Phys. **107**, 013704 (2010); 10.1063/1.3270431

[Recombination kinetics of Te isoelectronic centers in ZnSTe](#)

Appl. Phys. Lett. **86**, 052107 (2005); 10.1063/1.1861128

[Intensity dependence and transient dynamics of donor–acceptor pair recombination in ZnO thin films grown on \(001\) silicon](#)

Appl. Phys. Lett. **82**, 2290 (2003); 10.1063/1.1566482

The advertisement features a dark blue background with white and orange text. At the top left, it reads 'NEW! Asylum Research MFP-3D Infinity™ AFM' in large white letters, followed by 'Unmatched Performance, Versatility and Support' in orange. On the right, the Oxford Instruments logo is shown with the tagline 'The Business of Science®'. Below the text are four images: a blue textured surface, a brown textured surface, a grid of colorful squares, and the MFP-3D Infinity AFM instrument itself. Text descriptions are placed around these images: 'Stunning high performance' (top left), 'Simpler than ever to GetStarted™' (top right), 'Comprehensive tools for nanomechanics' (bottom left), and 'Widest range of accessories for materials science and bioscience' (bottom right).

Temperature-dependent decay dynamics in highly mismatched ZnSe_{1-x}Te_x alloy

Yan-Cheng Lin,^{1,a)} Wei-Shi Jiang,¹ Wu-Ching Chou,^{1,a)} Wei-Kuo Chen,¹ Wen-Hao Chang,¹ Chin-Hau Chia,² Cheng-Yu Chen,³ and Jen-Inn Chyi³

¹Department of Electrophysics, National Chiao Tung University, Hsinchu 30010, Taiwan

²Department of Applied Physics, National University of Kaohsiung, Kaohsiung 81148, Taiwan

³Department of Electrical Engineering, National Central University, Zhongli 32001, Taiwan

(Received 26 October 2011; accepted 1 February 2012; published online 17 February 2012)

This study investigates the temperature-dependent decay dynamics in highly mismatched ZnSe_{0.950}Te_{0.050} alloy using photoluminescence (PL) and time-resolved PL spectroscopy. The PL peak energy exhibits a *V-shaped* dependence on temperature (10–300 K), indicating strong carrier localization. Kohlrausch's stretched exponential law, in which the deduced stretching exponent β is highly consistent with the *V-shaped* PL peak shift, closely corresponds to the complex decay curves over a wide temperature range. Additionally, the PL lifetime τ initially increases and then monotonically declines as the temperature increases. These findings agree excellently with the low *electron-hole* binding energy upon thermal ionization of weakly bound electrons. © 2012 American Institute of Physics. [doi:10.1063/1.3687187]

Highly mismatched alloys (HMAs), whose fundamental properties are drastically modified through the substitution of a relatively small fraction of host atoms with those of an element of a distinctly different size and electronegativity, are currently attracting considerable interest. ZnSe_{1-x}Te_x and ZnSe_{1-x}O_x are well-known examples of II-VI HMAs, exhibiting giant band gap bowing and reductions in both pressure-dependence and temperature-dependence of the band gaps.¹⁻⁵ These unusual properties are well explained in the framework of the band anticrossing (BAC) model.^{6,7} According to this model, the electronic structure of the alloys is determined by the interaction between defect states introduced by the minority Te or O atoms and the extended states of the host semiconductor matrix. As a result, the conduction band (CB) or the valence band (VB) splits into two subbands (E_+ and E_-) with distinctly nonparabolic dispersion relations.⁶ Since the electronegativity of the incorporated Te/O atom is less/greater than that of the host Se atom, isovalent defect states form near the VB edge (VBE)/CB edge (CBE). Accordingly, the interactions that occur in ZnSe_{1-x}Te_x and ZnSe_{1-x}O_x are thought to be VB anticrossing (VBAC) and CB anticrossing (CBAC), respectively. Although extensive effort has been made to engineer the band gaps of ZnSe_{1-x}Te_x and ZnSe_{1-x}O_x, the recombination dynamics and carrier lifetimes in these complex systems have seldom been addressed. We have shown recently that the mechanism of carrier recombination in ZnSe_{0.947}O_{0.053} undergoes a complex change from one that involves trapped excitons to one that involves free excitons, causing an *S-shaped* photoluminescence (PL) peak shift and a monotonic decrease in PL lifetime with increasing temperature.⁵ The incorporation of Te and O generates hugely distinct localization energies and band anticrossing structures in ZnSe,¹⁻³ in which dissimilar temperature-dependent carrier dynamics in ZnSe_{1-x}Te_x from that in ZnSe_{1-x}O_x are expected. This study explores compre-

hensively the decay dynamics in ZnSe_{0.950}Te_{0.050} by using temperature-dependent PL and time-resolved PL (TRPL) spectroscopy. In contrast to ZnSe_{0.947}O_{0.053}, ZnSe_{0.950}Te_{0.050} exhibits clear changes in temperature-dependence of the PL peak energies and PL lifetimes.

ZnSe_{0.950}Te_{0.050} film with thickness of $\sim 0.5 \mu\text{m}$ was grown by molecular beam epitaxy on (001) GaAs substrate. The Te content was determined by energy-dispersive x-ray analyses. PL and TRPL were excited using a 200 ps pulsed laser diode (405 nm/2.5 MHz/1 mW). The PL and TRPL signals were dispersed using a 0.55 m spectrometer and detected using a multichannel LN₂-cooled charge-coupled device and a photon-counting avalanche photodiode. The decay traces were recorded using a time-correlated single photon counting approach (Time-Harp, PicoQuant). PL excitation (PLE) was conducted using an Xe lamp and dispersed by a 0.32 m monochromator.

Excitation power-dependent PL measurements of ZnSe_{0.950}Te_{0.050} at 10 K show a redshift and an asymmetric linewidth broadening of the PL peak as the laser power decreases. The PL peaks shift by about 23 meV as the laser power is decreased by three orders of magnitude. A ZnSe reference sample exhibited no change in peak position over the same decrease in power. The decrease in PL peak energy as the power decreases indicates that the density of states exhibits an exponential tail, which is formed by Te clustering or alloy fluctuations, thus implying possible carrier localization. Local regions of higher Te concentration are associated with lower energy states. These phenomena can be observed from the temperature-dependent PL spectra of ZnSe_{0.950}Te_{0.050}, which are presented in Fig. 1.

Figure 1(a) shows the temperature-dependent PL spectra of ZnSe_{0.950}Te_{0.050} with the indicated peak positions. At low temperatures (<140 K), the PL peaks shift monotonically toward lower energies as the temperature increases; these shifts are accompanied by asymmetric linewidth broadening. This behavior can be understood in terms of exciton localization in a variable potential that is formed by the distribution of Te

^{a)}Authors to whom correspondence should be addressed. Electronic addresses: bryanlin@mail.nctu.edu.tw and wuchingchou@mail.nctu.edu.tw.

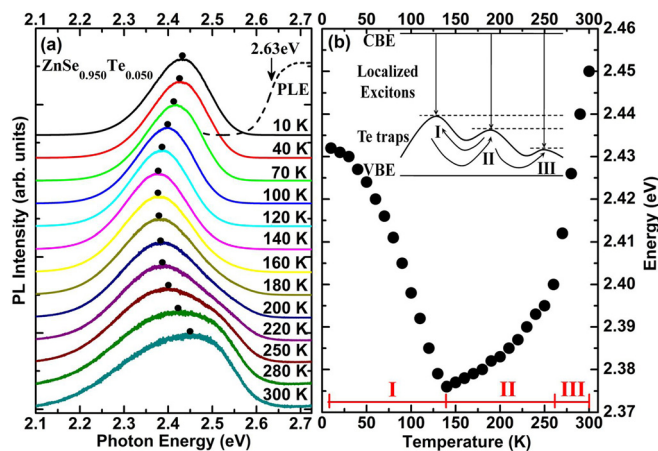


FIG. 1. (Color online) (a) Temperature-dependent PL spectra of $\text{ZnSe}_{0.950}\text{Te}_{0.050}$ and (b) corresponding PL peak energy versus temperature. Dashed curve in (a) is PLE spectrum of $\text{ZnSe}_{0.950}\text{Te}_{0.050}$, detected at the PL peak and 10 K. The black arrow indicates the band edge. Inset in (b) schematically depicts carrier decay paths; only three trap states are considered for simplicity.

atoms. Above 140 K, a pronounced blueshift of the peak is observed as the temperature increases, and a high energy shoulder appears, causing significant PL linewidth broadening. Figure 1(b) plots the temperature-dependent PL peak energies, determined from Fig. 1(a). The PL peaks exhibit a *V-shaped* (redshift-blueshift) energy shift as the temperature increases. As compared with the *S-shaped* (redshift-blueshift-redshift) energy shift of $\text{ZnSe}_{0.947}\text{O}_{0.053}$ [in which electrons are delocalized in the free state at high temperatures owing to the small localization energy (~ 20 meV)],⁵ the *V-shaped* energy shift of $\text{ZnSe}_{0.950}\text{Te}_{0.050}$ over the same range of temperatures (10–300 K) implies a rather deep localization (in which the holes are still localized in Te trap states at room temperature). From the PLE spectrum of $\text{ZnSe}_{0.950}\text{Te}_{0.050}$ detected at the PL peak (2.43 eV) and at 10 K, it is clear that this emission is preferentially excited via band-to-band proc-

esses. Additionally, a large Stokes shift of ~ 200 meV from the band edge (~ 2.63 eV) is measured by PLE. This value matches the PL binding energy ($E_g - E_{PL}$) obtained elsewhere,¹ verifying that the emissions within the specified temperature range are all caused by localized excitons.

To gain insight into the decay dynamics of $\text{ZnSe}_{0.950}\text{Te}_{0.050}$, Fig. 2(a) shows the temperature-dependent TRPL spectra. Clearly, many interesting conclusions can be drawn. (i) As the temperature increases up to 70 K, the PL lifetime (τ) increases; as the temperature increases further, τ monotonically declines. (ii) None of the PL decay profiles exhibits monoexponential decay. (iii) All of the TRPL spectra (10–180 K) on a double logarithmic scale are straight lines [inset in Fig. 2(a)], which are strong evidence that the PL decay profiles of $\text{ZnSe}_{0.950}\text{Te}_{0.050}$ follow the Kohlrausch's stretched exponential law.³ These facts demonstrate peculiar and complex carrier dynamics in $\text{ZnSe}_{0.950}\text{Te}_{0.050}$. Hence, the decay curves of $\text{ZnSe}_{0.950}\text{Te}_{0.050}$ are all fitted using the stretched exponential function,³ $I(t) = I_0 \cdot e^{-(t/\tau)^\beta}$, where β is the stretching exponent and reflects the relaxation rates involved in the decay process. The gradient of the TRPL data on a double logarithmic scale, as plotted in the inset, yields β .

Figures 2(b) and 2(c) plot the measured PL lifetime τ and β versus temperature for $\text{ZnSe}_{0.950}\text{Te}_{0.050}$, respectively. Unlike PL lifetime τ , β initially decreases with increasing temperature to a minimum at 140 K, and then increases with a further increase in temperature. Notably, the kink in β appears at 140 K, which is consistent with that in the *V-shaped* curve of PL peak energies in Fig. 1(b). The configuration relaxation model that is shown in the inset in Fig. 1(b) explains this phenomenon. At 10 K, the photoexcited holes are localized in the nearest potential trap states whereas electrons are more weakly bound by a Coulomb force, causing the average optical transition energy of the localized exciton peak to be lower than the low-temperature band gap measured by PLE. The initial decrease in β is

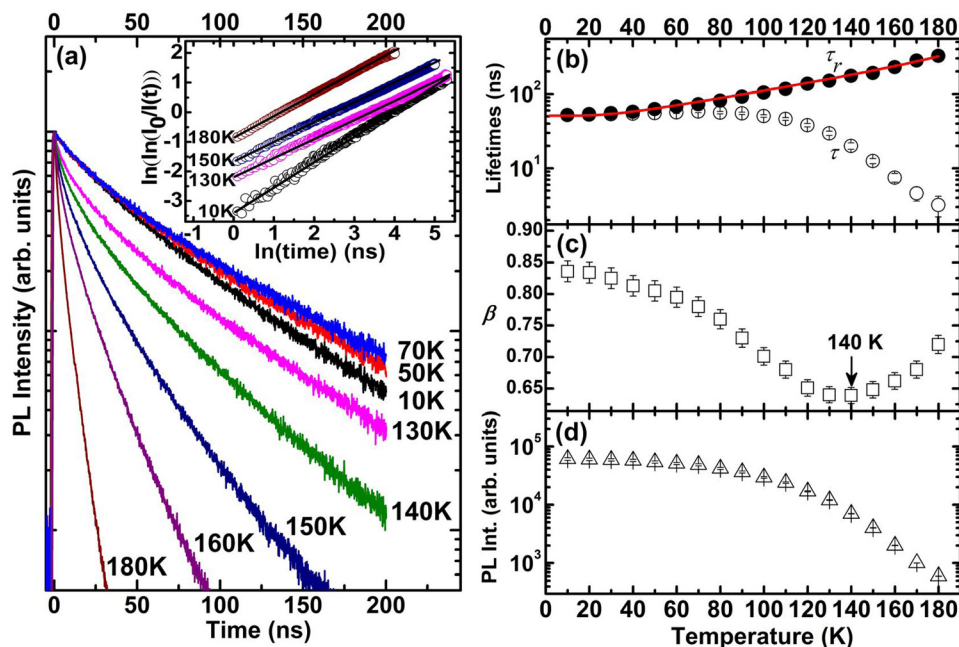


FIG. 2. (Color online) Temperature-dependent (a) TRPL spectra, (b) PL lifetime τ (open circles) and radiative lifetime τ_r (solid circles), (c) stretching exponent β , and (d) integrated PL intensity I_{PL} of $\text{ZnSe}_{0.950}\text{Te}_{0.050}$. Inset in (a) shows TRPL spectra on a double logarithmic scale. The solid line in (b) is the fitting result of τ_r using Eq. (1).

attributed to the increase in the number of additional recombination paths for the excitons as the temperature increases, because these less mobile holes gain extra energy that enables them to transfer to deeper Te traps (path I), causing a rapid redshift in the PL peak. Simultaneously, as the temperature approaches 140 K, some of the trapped holes are thermally activated to repopulate states of higher energy. Therefore, the PL linewidth increases at the high energy shoulder, and both PL peak energy and β reach their local minima there. The further reduction of β herein is caused by the coexistence of two directional carrier transfers. However, as the temperature increases further, an increasing number of holes gain enough energy to transfer to states of higher energy (path II) and recombine. Thus, the recombination from path I gradually disappears, increasing β and causing a blueshift in the PL peaks. Above 260 K, holes suddenly move up to higher-energy states (path III) with an energy that differs from that associated with path II, causing a sharp PL peak blueshift. The TRPL images of ZnSe_{0.950}Te_{0.050} at 10 K and 160 K, shown in Figs. 3(a) and 3(b), further confirm the aforementioned carrier effects. At 10 K, the emission peak shifts monotonically to lower energy over time. However, this redshift of the emission eventually ends and is replaced by a shift toward higher energies at 160 K. The phenomenon becomes even more pronounced at higher temperatures.

The initial increase in PL lifetime τ , shown in Fig. 2(b), is readily understood as follows. In ZnSe_{0.950}Te_{0.050}, holes hop among proximal Te traps and remain much more tightly bound than electrons. As the temperature rises, electrons tend to reach an equilibrium distribution between the positively charged Te traps and the CB. Therefore, the weakly bound electrons are ionized and move away from the strongly localized holes for an increasing proportion of their lifetimes, extending the radiative lifetime (τ_r). This explanation applies only if the nonradiative processes are negligible, which they are, as confirmed by the almost constant integrated PL intensity (I_{PL}) in the same temperature region [Fig. 2(d)], because the measured PL lifetime τ comprises both radiative (τ_r) and nonradiative (τ_{nr}) components and is given by $\tau^{-1} = \tau_r^{-1} + \tau_{nr}^{-1}$. A standard way to extract τ_r from the measured PL lifetime τ is to determine the radiative efficiency $\eta(T) = \tau_{nr}/(\tau_{nr} + \tau_r)$. From the measured

temperature-dependent I_{PL} , τ_r can be determined using $\tau_r(T) = \tau(T)/\eta(T)$, by assuming $\eta(T) = I_{PL}(T)/I_{PL}(10K)$.

The derived temperature-dependent radiative lifetimes (τ_r) are also plotted in Fig. 2(b) and fitted using the following equation:⁸

$$\tau_r(T) = \tau_r(0)/[1 - \chi(T)], \quad (1)$$

where $\chi(T) = C \exp(-\varepsilon_{e-h}/kT)$ is the probability that a center is ionized by loss of an electron; $\tau_r(0)$ is the radiative lifetime at $T=0$ K; C is a constant; ε_{e-h} is a characteristic energy that is of the order of the *electron-hole* (*e-h*) binding energy, and k is the Boltzmann constant. The fitting results yield $\tau_r(0) = 51.2 \pm 0.3$ ns, $C = 1.46 \pm 0.02$, and $\varepsilon_{e-h} = 8.6 \pm 0.1$ meV. Such a low *e-h* binding energy in this temperature range is highly consistent with the increase in τ_r upon the thermal ionization of electrons. However, as the temperature increases, the lifetime time difference between the PL lifetime τ and the radiative lifetime τ_r is associated with the fact that the nonradiative recombination starts to affect the PL decay.

The carrier dynamics of ZnSe_{0.950}Te_{0.050} discussed herein exhibit various dissimilarities with those of ZnSe_{0.947}O_{0.053}.⁵ The PL peak energy of ZnSe_{0.950}Te_{0.050} exhibits a *V-shaped* shift, while that of ZnSe_{0.947}O_{0.053} exhibits an *S-shaped* shift. Increasing the temperature initially increases the PL lifetime τ of ZnSe_{0.950}Te_{0.050} to 70 K, with a nearly constant I_{PL} . However, both the PL lifetime τ and the I_{PL} of ZnSe_{0.947}O_{0.053} decrease monotonically as the temperature increases.⁵ These inconsistencies are attributed to the distinctly different localization energies and BAC structures of ZnSe_{0.950}Te_{0.050} and ZnSe_{0.947}O_{0.053}. The localization energy is associated with the energy difference between isovalent Te/O trap states ($E_{Te}^{trap}/E_{O}^{trap}$) and the new VB edge (E_+)/CB edge (E_-). In ZnSe_{1-x}O_x, since the O defect state is above the CB of ZnSe, the BAC interaction causes the formation of a relatively wide lower E_- subband and a smaller localization energy ($E_- - E_O^{trap} \sim 20$ meV).^{5,7} However, the BAC model predicts that a narrow lower E_+ subband is formed in ZnSe_{1-x}Te_x, resulting in a larger localization ($E_{Te}^{trap} - E_+ \sim 200$ meV) because the Te defect state arises above the VB of ZnSe (inside the band gap).^{2,3,7} Moreover, ZnSe is intrinsically n-type and holes are its minority carriers. For ZnSe_{0.950}Te_{0.050}, the minority carriers are trapped and tightly bound to the Te atoms due to VBAC. Hence, the electrons are much more easily thermally ionized and able to move away from the trapped holes. However, owing to CBAC, O atoms trap the majority carriers and the minority holes are tightly bound in ZnSe_{0.947}O_{0.053}, causing the decay dynamics to differ markedly from those of ZnSe_{0.950}Te_{0.050}.

In summary, this study investigated the decay dynamics in ZnSe_{0.950}Te_{0.050} HMA as a function of temperature. The *V-shaped* dependence of the PL peak energy implies that localized excitons, in which the holes are deeply trapped, dominate all optical transitions from 10 to 300 K. The relaxation model that is based on the deduced temperature-dependent β and *V-shaped* PL peak energy clarifies clearly the complicated carrier recombination. Initially, PL lifetime τ increases with temperature up to 70 K, with almost

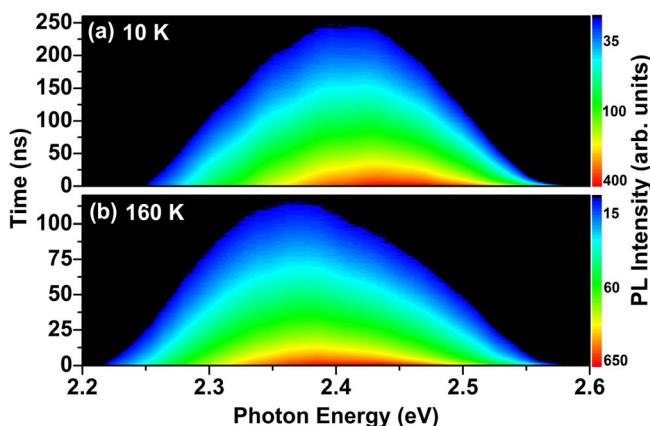


FIG. 3. (Color online) TRPL images of ZnSe_{0.950}Te_{0.050} at (a) 10 K and (b) 160 K.

constant I_{PL} , reflecting a prolonged radiative lifetime τ_r . These results are further supported by the derived e - h binding energy ($\varepsilon_{e-h} \sim 8.6$ meV), which is associated with the thermal ionization of weakly bound electrons. The experimental results indicate that the carrier dynamics and decay lifetimes of HMAs can be engineered further by additional electron or hole doping.

This work was supported by the Ministry of Education and the National Science Council under Grant No. NSC 100-2119-M-009-003.

¹M. J. S. P. Brasil, R. E. Nahory, F. S. Turco-Sandroff, H. L. Gilchrist, and R. J. Martin, *Appl. Phys. Lett.* **58**, 2509 (1991).

- ²J. Wu, W. Walukiewicz, K. M. Yu, J. W. Ager III, E. E. Haller, I. Miotkowski, A. K. Ramdas, C. H. Su, I. K. Sou, R. C. C. Perera *et al.*, *Phys. Rev. B* **67**, 035207 (2003).
- ³Y. C. Lin, W. C. Chou, W. C. Fan, J. T. Ku, F. K. Ke, W. J. Wang, S. L. Yang, W. K. Chen, W. H. Chang, and C. H. Chia, *Appl. Phys. Lett.* **93**, 241909 (2008).
- ⁴W. Shan, W. Walukiewicz, J. W. Ager III, K. M. Yu, J. Wu, E. E. Haller, Y. Nabetani, T. Mukawa, Y. Ito, and T. Matsumoto, *Appl. Phys. Lett.* **83**, 299 (2003).
- ⁵Y. C. Lin, H. L. Chung, W. C. Chou, W. K. Chen, W. H. Chang, C. Y. Chen, and J. I. Chyi, *Appl. Phys. Lett.* **97**, 041909 (2010).
- ⁶W. Shan, W. Walukiewicz, J. W. Ager III, E. E. Haller, J. F. Geisz, D. J. Friedman, J. M. Olson, and S. R. Kurtz, *Phys. Rev. Lett.* **82**, 1221 (1999).
- ⁷J. Wu, W. Shan, and W. Walukiewicz, *Semicond. Sci. Technol.* **17**, 860 (2002).
- ⁸J. D. Cuthbert and D. G. Thomas, *Phys. Rev.* **154**, 763 (1967).